

Curve Reconstruction from Noisy and Unordered Samples

Marek W. Rupniewski

Institute of Electronic Systems, Warsaw University of Technology, Nowowiejska 15/19, 00-665 Warsaw, Poland

Keywords: Curve Reconstruction, Noisy Samples.

Abstract: An algorithm for the reconstruction of closed and open curves from clouds of their noisy and unordered samples is presented. Each curve is reconstructed as a polygonal path represented by its vertices, which are determined in an iterative process comprising evolutionary and decimation stages. The quality of the reconstruction is studied with respect to the local density of the samples and the standard deviation of the noise perturbing the samples. The algorithm is verified to work for arbitrary dimensions of ambient space.

1 INTRODUCTION

In many engineering problems, there is a need to fit a curve to an irregularly spaced set of points. Typically, these problems fall into one of the following categories. If the ordered points lie exactly on the curve to be found, then one deals with an interpolation problem. If the points still lie on the curve, but their order on the curve is unknown, then one must recover the order prior to interpolation. For this task, one may use e.g. the algorithms presented in (Gold and Snoeyink, 2001), (Dey et al., 2000), (Althaus and Mehlhorn, 2001). If one knows the order of the points along the curve, but the points are disturbed by the noise, then one approximates the curve usually with some kind of splines, see e.g. (Cohen and O'Dell, 1989), (Fritsch and Carlson, 1980), (Hözlze, 1983). Finally, one may face a problem where both the noise is present, and the order of the sample points along the curve is unknown. This kind of problem appears in Computed Axial Tomography (CAT), Coordinate-Measuring Machine (CMM) measurements and Magnetic Resonance Imaging (MRI). In the literature, there are given various strategies to solve the problems falling into this class. Fang and Gossard (Fang and Gossard, 1995) proposed fitting a curve with given end-points by minimizing some spring energy function. Goshtasby (Goshtasby, 2000) obtained a reconstruction by tracing ridges of a certain inverse distance function (for this, he needed to evaluate the function on a dense grid). A pixel-based solution was proposed by Pottmann and Randrup (Pottmann and Randrup, 1998). They recovered a curve as a medieval line of a set of pixels (of appro-

priate size) that cover the points. There is also an approach to the problem based on moving least-square method showed by Levin (Levin, 1998) and improved by Lee (Lee, 2000). A more statistic point of view led Hastie and Stuetzle (Hastie and Stuetzle, 1989) towards the reconstruction of the unknown curve as a principal curve of the given set of points. Finally, let us mention the work of Cheng et al. (Cheng et al., 2005) in which a curve was reconstructed by determining and following a minimum width strip containing the noisy points.

The way we solve the problem of curve reconstruction starts with a choice of a number of balls centered at the curve samples. Then, in each iteration, the balls are moved (hopefully towards the original curve) and their number is reduced in such a way that they do not overlap too much. Eventually, the balls' centers are ordered and then claimed to be consecutive vertices of a polygonal path approximating the curve being recovered (see Fig. 1 for an example of the cloud of samples and a result of the reconstruction algorithm).

The obtained polygonal path, being an approximation itself, may also play a role of an "initial guess" that is fundamental for the success of more sophisticated reconstruction algorithms (see e.g. (Ruiz et al., 2013)). One may also use the obtained vertices for construction of a smooth, instead of a polygonal, approximation based, for example, on splines or rational Gaussian curves (Goshtasby, 1995).

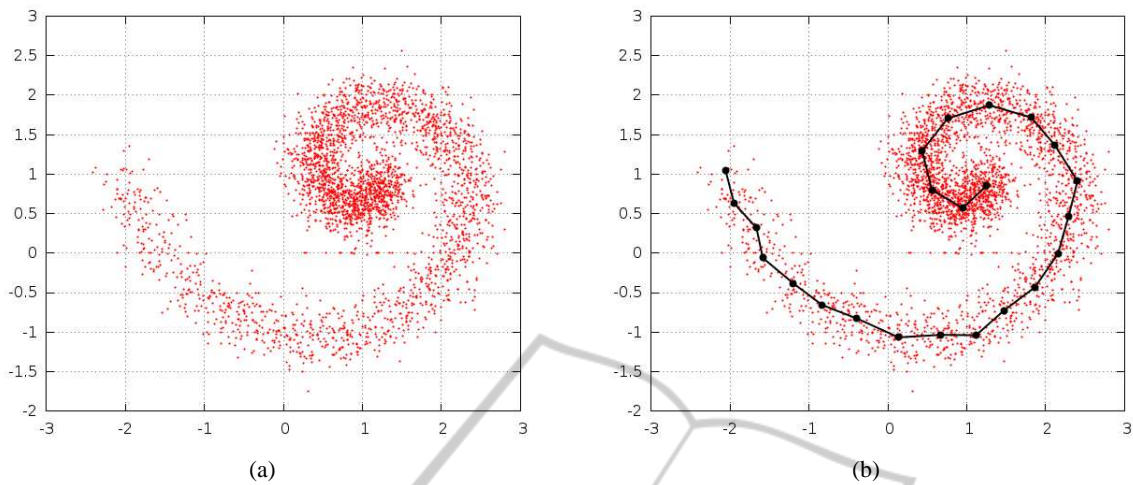


Figure 1: A set D of noisy samples of an unknown curve (Subfig. 1(a)) and a reconstruction (solid line on Subfig. 1(b)) resulted from D .

2 PROBLEM STATEMENT

The aim is to recover a piece-wise smooth curve $\gamma \subset \mathcal{R}^d$ given a set of curve samples that are affected by some noise. We will assume that the samples are independent, i.e. that they form a set D of realizations of identically distributed and independent random variables with some probability density function $f: \mathcal{R}^d \rightarrow \mathcal{R}$, which has its support located along curve γ .

By recovering curve γ from set D we mean constructing a polygonal path (determined by the sequence of its vertices) that approximates γ . The quality of this approximation may be assessed by the Hausdorff distance d between the polygonal path $\hat{\gamma}$ and curve γ :

$$d(\gamma, \hat{\gamma}) = \max \left(\max_{p \in \hat{\gamma}} \min_{q \in \gamma} \|p - q\|, \max_{p \in \gamma} \min_{q \in \hat{\gamma}} \|p - q\| \right).$$

Of course to perform such an assessment one needs to know γ , which is rarely the case except for simulations.

The quality of curve reconstruction depends upon many factors:

- the number of samples n ,
- their distribution along curve γ ,
- the distribution of sample errors,
- the dimension d of the ambient space \mathcal{R}^d ,
- the curvature of the curve.

In section 4, the quality of the reconstruction is studied in the case of uniform distribution of the samples with respect to the arc length of the curve, normal

distribution of the sample errors and negligible curvature.

3 ALGORITHM

The algorithm for curve reconstruction consists of four steps (two of which are repeated in a loop) and is presented in Fig. 2. The result of the algorithm is a set E of pairs of the end-points of line segments comprising a polygonal path approximating the curve.

Require: a non-empty set $D \subset \mathcal{R}^d$ of noisy samples of an unknown curve γ and a parameter $R > 0$

```

S ← choose(D, R)
repeat
    S ← evolve(S, D, R)
    S ← decimate(S, R)
until S is not affected by the last decimation
E ← order(S, R)
    
```

Figure 2: The algorithm for curve reconstruction.

3.1 Initialization

In the first step of the algorithm

$$S \leftarrow \text{choose}(D, R)$$

an initial set S of the path's nodes is chosen. For simplicity, we propose taking for S a randomly chosen R -separated subset of the sample set D , where by R -separated set we mean a set having no two different points closer than R .

3.2 Evolution

The heart of the curve reconstruction algorithm is the evolution of the set S

$$S \leftarrow \mathbf{evolve}(S, D, R).$$

The aim of the evolution is to move the points belonging to S towards the curve being reconstructed and spread them along this curve. The evolution algorithm is presented in Fig. 3.

```

repeat
   $Q \leftarrow S$ 
   $S \leftarrow \{\text{avg}(D \cap \text{vcell}(p, Q, R)) \mid p \in Q\}$ 
until  $Q = S$ 

```

Figure 3: Function $Q = \mathbf{evolve}(S, D, R)$. $\text{avg}(X)$ denotes the mass centre of the points from $X \subset \mathcal{R}^d$.

In each step of the evolution, every node $p \in S$ is moved to the mass centre of the points from D falling into the intersection $\text{vcell}(p, S, R)$ of the ball of radius R centered at p and the p 's cell of the Voronoi diagram constructed for S , i.e.,

$$\text{vcell}(p, S, R) = \left\{ q \in \mathcal{R}^d \mid \forall_{o \in S} R \geq \|p - q\| \leq \|p - o\| \right\}, \quad (1)$$

where $\|x\|$ denotes the Euclidean norm of $x \in \mathcal{R}^d$. In Fig. 4 an example of the four-point node set is presented and the related intersections are depicted with various gray levels.

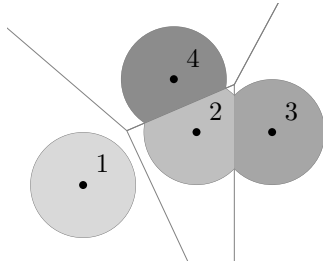


Figure 4: The cells (see eq. (1)) constructed for a four-point node set S . Each cell is the intersection of a ball centered at a point, and this point's Voronoi cell of the Voronoi diagram constructed for S .

Moving a point towards the mass center of its small circular neighbourhood accounts for convergence towards the region of bigger mass density (we assume that the closer is a point to the curve being reconstructed, the bigger is the probability of having a sample falling into the neighbourhood of the point). Restricting the circular neighbourhoods to the Voronoi cells prevents the points from concentrating around single points of the curve.

```

while  $\#S > 3$  and there are points  $p \in S$  satisfying
condition (2) do
  remove from  $S$  a randomly chosen point  $p$  satisfying (2)
end while

```

Figure 5: Function $S \leftarrow \mathbf{decimate}(S, R)$.

3.3 Decimation

The decimation step

$$S \leftarrow \mathbf{decimate}(S, R)$$

of the algorithm is responsible for the reduction of the number of points in S . Thus, it directly affects the rate of convergence of the algorithm, the robustness of the algorithm with respect to outliers, and the ability of the algorithm to cope with curve self-intersections, its end-points, and other singularities (in case there are any).

In this paper, we present an algorithm for reconstruction of smooth curves without self-intersections. Therefore, we propose quite a simple decimation algorithm presented in Fig. 5. In its formulation, the statement that $p \in S$ satisfies condition (2) means that p has more than two other points from S in its $2R$ -neighbourhood or it has less than two other points from S in its $4R$ -neighbourhood, i.e.,

$$\#\{q \in S \mid \|p - q\| \leq 2R\} > 3 \quad \text{or} \\ \#\{q \in S \mid \|p - q\| \leq 4R\} < 3. \quad (2)$$

3.4 Ordering

During the ordering step

$$E \leftarrow \mathbf{order}(S, R)$$

the points belonging to set S are ordered so that two consecutive points on the polygonal path are consecutive in sequence E . One can think of this stage as of joining points of S with line segments in order to obtain a polygonal path (open or closed). A line segment may be represented with the set of its two end-points. The algorithm for identifying all such segments is presented in Fig. 6. The algorithm is designed so that it can produce more than one path in case the samples origin from more than one curve.

4 SIMULATION

To assess the quality of the reconstruction algorithm the following simulations were performed. Samples

```

E ← { {p, q} ⊂ S | p ≠ q and ||p - q|| ≤ 2R }
while there are points p, q ∈ S such that each of
them appears in at most one pair comprising set E
and ||p - q|| ≤ 4R do
    E ← E ∪ { {p, q} }
end while
    
```

Figure 6: Function $E \leftarrow \text{order}(S, R)$.

of a line segment $I = [0, 100] \times \{0\} \subset \mathcal{R}^2$ were chosen according to uniform distribution, and then they were perturbed by standard normal deviates. Please note that this is also a model for situation, in which the original curve has some non-zero curvature but the radius of this curvature is much bigger than the standard deviation of the noise (locally, after proper scaling, the curve looks like a line segment and the deviates become standard). For various values of the algorithm parameter R and for various number ρ of samples per unit length line segment, the following outputs of the algorithm were gathered:

- the median of the distances between the polygonal path vertices and line segment I ,
- the maximum of the distances between the polygonal path vertices and line segment I ,
- the bigger of the distances between the polygonal path and the end-points of I .

The maximum of the latter two quantities forms the Hausdorff distance between polygonal path and the line segment being reconstructed. The experiments were repeated 100 times for each set of parameters in order to estimate the mean value and the quartiles for the above quantities. The results are presented in Fig. 8.

According to this figure, for a given number of samples (per unit length curve segment) and the deviation of the noise, the radius R should be neither too small nor too big. The small values of R do not allow points of S to evolve towards the segment, while the big values of R results in worse approximation of the end-points of the segment. We can also observe that the distance between the polygonal path vertices and the line segment decrease with the number of samples (this decrease is almost linear for big numbers of samples), while the distance from these vertices to the end-points of the segment tends to a non-zero value that depends on parameter R .

4.1 Higher Dimensions

To verify that the algorithm produces desired results for dimensions of the ambient space bigger than two, another set of experiments was conducted. Samples

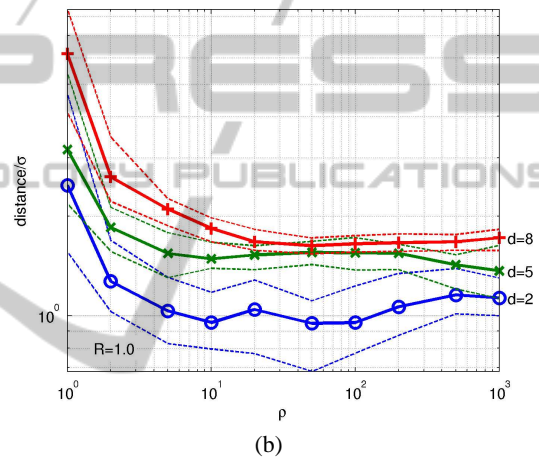
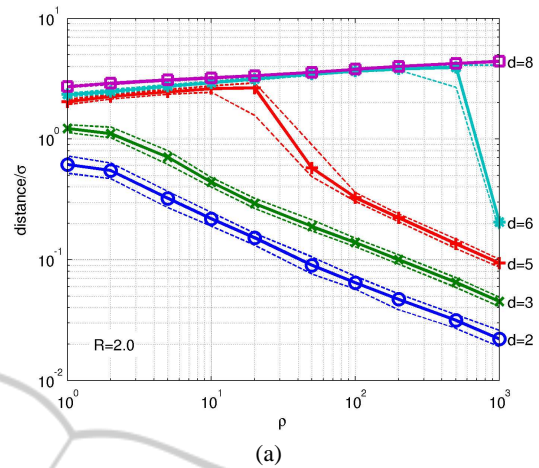


Figure 7: Results of reconstructions of a line segment lying in a d -dimensional space. Subfig. 7(a) shows estimated quartiles and median distance between reconstructed polygonal path vertices and the line segment. The median is depicted with a solid line, while the lower and the upper quartiles are shown with the dashed lines. Subfig. 7(b) shows estimates of the bigger of the two distances between an end-point of the segment and the set of the path vertices. In the both cases σ denotes the standard deviation of the normal noise perturbing the samples.

of a line segment

$$I = [0, 100] \times \{0\}^{d-1} \subset \mathcal{R}^d.$$

were perturbed by standard normal deviates. The parameter R of the reconstruction algorithm was fixed, and a number of reconstructions were performed for various values of the dimension d and various densities ρ of samples per unit length line segment. The resulting characteristics are shown in Fig. 7.

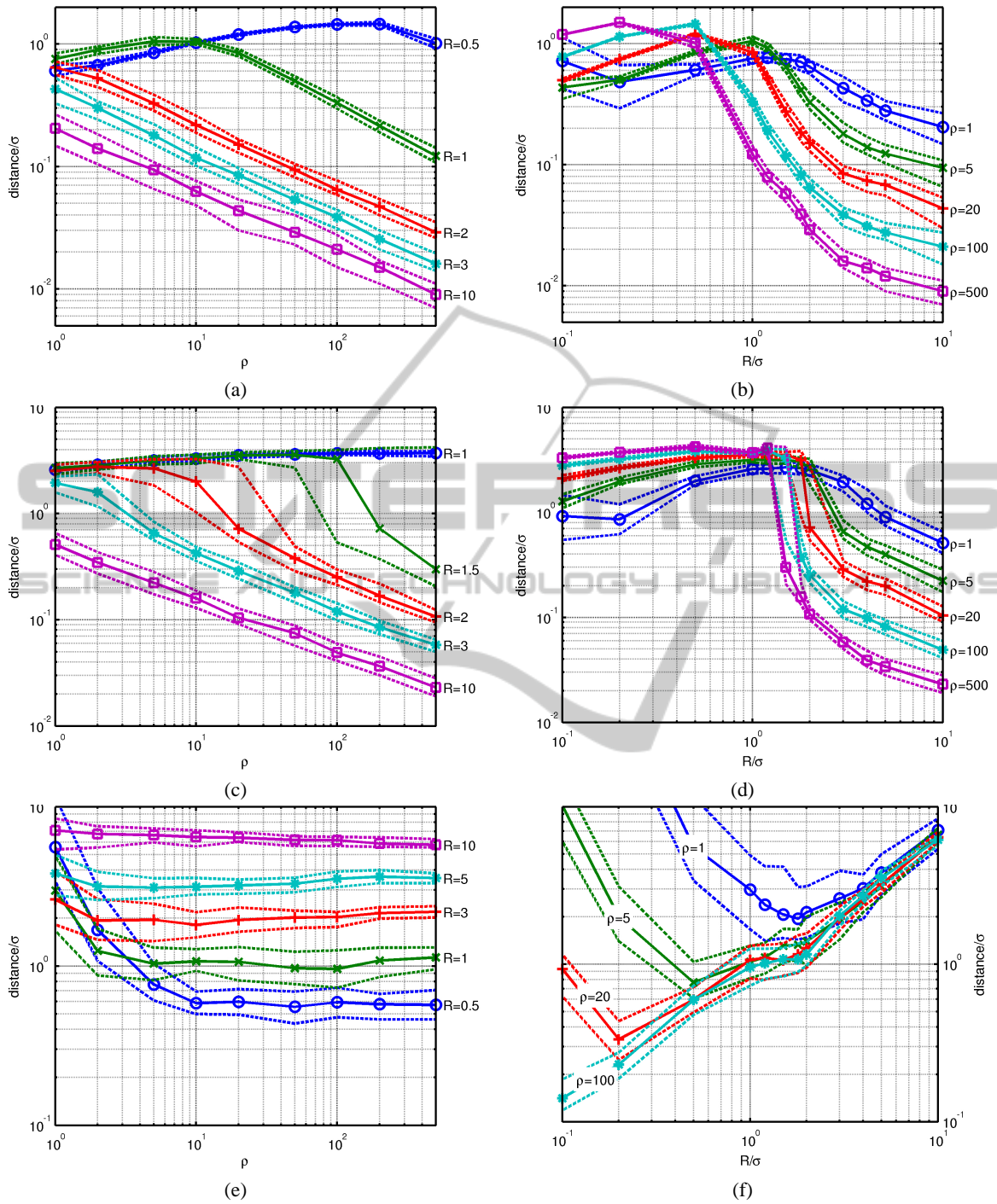


Figure 8: Results of reconstructions of a line segment (lying in \mathcal{R}^2) from its samples disturbed by normal deviates with standard deviation σ . ρ stands for mean number of samples per unit length line segment. In Subfig. 8(a) and 8(b) the estimated median distance from polygonal path vertices to the segment is shown. In Subfig. 8(c) and 8(d) the estimated maximum of the same distance is presented. The last two subfigures show estimates of the bigger of the two distances between an end-point of the segment and the set of polygonal path vertices. In each figure, dashed lines show the lower and the upper estimated quartiles for the corresponding (by color) quantity.

5 APPLICATION

The presented algorithm has been successfully used for the purpose of air targets trajectory reconstruction from radar raw data. The data comprised range bins at which the recorded signal exceeded a given threshold. The original data and the result of trajectory reconstruction are presented in Fig. 9.

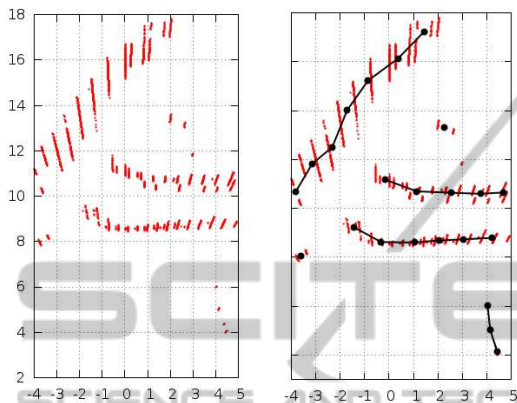


Figure 9: Air target reconstruction from raw radar data (the axes are scaled in kilometers; the right Figure was obtained with the algorithm for $R = 0.9\text{km}$).

6 CONCLUSIONS

In this paper we have presented a novel algorithm for the reconstruction of a curve from a cloud of its noisy and unordered samples. One of the merits of the algorithm is its simplicity – others include:

- no requirement of an initial guess for the reconstructed curve,
- the curve end-points don't need to be specified,
- its ambient space dimension is arbitrary,
- it works for both open and closed curves,
- it works for any number of disjoint curves.

The algorithm, in its presented form, does not cope with intersecting curves well. Research is being undertaken to improve it in this aspect. Also, we are working on adapting the algorithm to anisotropic data (e.g., location-time data points) and on automatic adaptation of parameter R .

ACKNOWLEDGEMENTS

This work has been supported by the National Center for Research and Development (NCBiR) under Grant No. DOBR/0041/R/ID1/2012/03.

REFERENCES

- Althaus, E. and Mehlhorn, K. (2001). Traveling salesman-based curve reconstruction in polynomial time. *SIAM Journal on Computing*, 31(1):27–66.
- Cheng, S.-W., Funke, S., Golin, M., Kumar, P., Poon, S.-H., and Ramos, E. (2005). Curve reconstruction from noisy samples. *Computational Geometry*, 31(12):63–100.
- Cohen, E. and O'Dell, C. (1989). A data dependent parametrization for spline approximation. *Mathematical Methods in Computer Aided Geometric Design*, pages 155–166.
- Dey, T., Mehlhorn, K., and Ramos, E. (2000). Curve reconstruction: Connecting dots with good reason. *Computational Geometry: Theory and Applications*, 15(4):229–244.
- Fang, L. and Gossard, D. C. (1995). Multidimensional curve fitting to unorganized data points by nonlinear minimization. *Computer-Aided Design*, 27(1):48–58.
- Fritsch, F. and Carlson, R. (1980). Monotone piecewise cubic interpolation. *SIAM J. Numer. Anal.*, 17(2):238–246.
- Gold, C. and Snoeyink, J. (2001). A one-step crust and skeleton extraction algorithm. *Algorithmica (New York)*, 30(2):144–163.
- Goshtasby, A. (1995). Geometric modelling using rational gaussian curves and surfaces. *Computer-Aided Design*, 27(5):363–375.
- Goshtasby, A. (2000). Grouping and parameterizing irregularly spaced points for curve fitting. *ACM Transactions on Graphics*, 19(3):185–203.
- Hastie, T. and Stuetzle, W. (1989). Principal curves. *Journal of the American Statistical Association*, 84(406):502–516.
- Hözlle, G. (1983). Knot placement for piecewise polynomial approximation of curves. *Computer-Aided Design*, 15(5):295–296.
- Lee, I.-K. (2000). Curve reconstruction from unorganized points. *Computer Aided Geometric Design*, 17(2):161–177.
- Levin, D. (1998). The approximation power of moving least-squares. *Mathematics of Computation*, 67(224):1517–1531.
- Pottmann, H. and Randrup, T. (1998). Rotational and helical surface approximation for reverse engineering. *Computing (Vienna/New York)*, 60(4):307–322.
- Ruiz, O. E., Cortés, C., Aristizábal, M., Acosta, D. A., and Vanegas, C. A. (2013). Parametric curve reconstruction from point clouds using minimization techniques. In *GRAPP/IVAPP*, pages 35–48.